HAL
archives-ouvertes.fr

New insights into the organisation and intracellular localisation of the two subunits of glucose-6-phosphatase.

Maud Soty, Julien Chilloux, Sylvie Casteras, Alexeï Grichine, Gilles Mithieux, Amandine Gautier-Stein

▶ **To cite this version:**

Maud Soty, Julien Chilloux, Sylvie Casteras, Alexeï Grichine, Gilles Mithieux, et al.. New insights into the organisation and intracellular localisation of the two subunits of glucose-6-phosphatase.. Biochimie, Elsevier, 2012, 94 (3), pp.695-703. 10.1016/j.biochi.2011.09.022 . inserm-00737760

HAL Id: inserm-00737760
https://www.hal.inserm.fr/inserm-00737760

Submitted on 4 Oct 2012

HAL is a multi-disciplinary open access archive for the deposit and dissemination of scientific research documents, whether they are published or not. The documents may come from teaching and research institutions in France or abroad, or from public or private research centers.

L'archive ouverte pluridisciplinaire **HAL**, est destinée au dépôt et à la diffusion de documents scientifiques de niveau recherche, publiés ou non, émanant des établissements d'enseignement et de recherche français ou étrangers, des laboratoires publics ou privés.

*Manuscript
Click here to download Manuscript: Soty M et al. 040811.doc
Click here to view linked References

New insights into the organisation and intracellular localisation of the two subunits of Glucose-6-phosphatase.

Maud Soty [a,b,c], Julien Chilloux [a,b,c], Sylvie Casteras [a,b,c], Alexeï Grichine [d], Gilles Mithieux [a,b,c] and Amandine Gautier-Stein [a,b,c].

[a] INSERM, Unit 855, Lyon, F-69008, France
[b] Université de Lyon, Lyon, F-69008, France
[c] Université de Lyon 1, Villeurbanne, F-69622, France
[d] Institut Albert Bonniot INSERM : U823, Université Joseph Fourier - Grenoble I, BP170, 38042 Grenoble Cedex 9,France

Address: Dr. Amandine Gautier-Stein,
INSERM U855, Faculté de Médecine Laennec,
8 rue G. Paradin,
69372 Lyon cedex 08

Tel. 0033478771064
Fax. 0033478778762
e-mail amandine.gautier-stein@univ-lyon1.fr

Abstract

Glucose-6 phosphatase (G6Pase), a key enzyme of glucose homeostasis, catalyses the hydrolysis of glucose-6 phosphate (G6P) to glucose and inorganic phosphate. A deficiency in G6Pase activity causes type 1 glycogen storage disease (GSD-1), mainly characterised by hypoglycaemia. Genetic analyses of the two forms of this rare disease have shown that the G6Pase system consists of two proteins, a catalytic subunit (G6PC) responsible for GSD-1a, and a G6P translocase (G6PT), responsible for GSD-1b. However, since their identification, few investigations concerning their structural relationship have been made.

In this study, we investigated the localisation and membrane organisation of the G6Pase complex. To this aim, we developed chimera proteins by adding a fluorescent protein to the C-terminal ends of both subunits. The G6PC and G6PT fluorescent chimeras were both addressed to perinuclear membranes as previously suggested, but also to vesicles throughout the cytoplasm. We demonstrated that both proteins strongly colocalised in perinuclear membranes. Then, we studied G6PT organisation in the membrane. We highlighted FRET between the labelled C and N termini of G6PT. The intramolecular FRET of this G6PT chimera was 27%. The coexpression of unlabelled G6PC did not modify this FRET intensity. Finally, the chimera constructs generated in this work enabled us for the first time to analyze the relationship between GSD1 mutations and the intracellular localisation of both G6Pase subunits. We showed that GSD1 mutations did neither alter the G6PC or G6PT chimera localisation, nor the interaction between G6PT termini. In conclusion, our results provide novel information on the intracellular distribution and organisation of the G6Pase complex.

Abbreviations:

CFP, cyan fluorescent protein; **ER,** endoplasmic reticulum; **FRET,** fluorescence resonance energy transfer; **FLIM**, fluorescence lifetime imaging; **G6P,** glucose-6 phosphate; **G6Pase,** glucose- 6 phosphatase; **G6PC,** G6Pase catalytic subunit; **G6PT,** G6P translocase; **GSD-1,** glycogen storage disease; **Pi,** inorganic phosphate; **YFP,** yellow fluorescent protein

1. Introduction

Glucose-6 phosphatase (G6Pase) catalyses the last enzymatic step before the release of glucose into the blood: the hydrolysis of glucose-6 phosphate (G6P) into glucose and inorganic phosphate (Pi). G6Pase activity is restricted to the liver [1], the kidney cortex [2] and the small intestine [3] and confers on these three organs the capacity to release glucose into the systemic circulation. This enzyme plays a key role in glucose homeostasis since a deficiency in G6Pase activity leads to a severe metabolic disorder mainly characterised by hypoglycaemia in the post-absorptive state: glycogen storage disease type 1 (GSD-1) [4]. From human genetic studies, GSD-1 patients have been classified in two types based on mutations of the *G6Pase catalytic subunit (g6pc)* or the *G6P translocase (g6pt)*. GSD-1a results from mutations in *g6pc* and GSD-1b from mutations in *g6pt*. Both proteins are thought to be anchored in the endoplasmic reticulum (ER) and also expressed in nuclear membranes [5]. This localisation was suggested from biochemical and histochemical studies based on phosphatase enzymatic activity [6-8]. However, no recent data based on the detection of G6Pase proteins have confirmed this intracellular localisation.

Since G6PC and G6PT are sufficient to completely account for G6Pase activity [9, 10], the current G6Pase substrate transport model proposes that the active site of G6PC is exposed to the ER lumen [11] and G6PT shuttles intracellular G6P across the ER membrane into the lumen, where it is hydrolysed. This model, based on two proteins, takes into account the kinetic characteristics of the G6Pase system. Indeed, in intact microsomal membranes (which correspond to an intact G6Pase system), G6P is specifically hydrolysed at a moderate rate and with high affinity. In solubilised ER membranes, in which catalytic activity is not dependent on substrate transport, G6Pase hydrolyses G6P at a high rate and affinity but, it decreases its substrate specificity and is therefore able to hydrolyse other sugar-6 phosphate moieties [12]. Moreover, disruption of microsomal membranes of livers from GSD-1b patients permits the recovery of normal G6Pase activity, whereas intact GSD-1b liver microsomes exhibit very low G6Pase activity [13, 14]. This set of data has suggested that G6PT is necessary for G6P transport in intact ER membranes and confers substrate specificity to the G6Pase system.

The importance of both proteins for optimal enzymatic activity has been confirmed in animal models. Using mice knocked out for *g6pc* (*g6pc*$^{-/-}$), Lei *et al.* have

suggested that a loss of *g6pc* gene expression annuls both G6P transport and hydrolysis [15]. In *g6pc*$^{-/-}$ mice, a single administration of an adenovirus containing the cDNA encoding *g6pc* (AdCMV-G6PC) improved the majority of GSD-1a metabolic abnormalities. The AdCMV-G6PC infusion restored 19% of normal G6Pase activity in the liver and, interestingly, corrected G6P transport deficiency in hepatic microsomes of *g6pc*$^{-/-}$ mice [16]. The same authors examined microsomal G6P transport in transient expression studies in COS-1 cells and have shown that G6P transport is increased in cells transfected with either the *g6pc* or *g6pt* cDNA compared with mock-transfected cells. Moreover, G6P transport was more efficient in cells which co-expressed both genes [17]. These studies provide direct evidence that G6PT and G6PC are tightly inter-dependent for global G6Pase activity.

Concerning their protein characteristics, neither proteins of the G6Pase system have been purified to homogeneity, but their individual structures within the membrane have been predicted using proteolytic digestion of tagged proteins [18, 19]. We have reported that [^{32}P]G6PC migrates at an apparent molecular mass of 37 kDa in SDS-PAGE under denaturing conditions. This is consistent with its molecular mass determined by immunoblotting [20]. Using radiation inactivation analysis, Ness *et al.* suggested that the molecular weight of functional G6Pase ranged around 75-100 kDa, in both intact and solubilised ER membrane [21]. These observations have suggested that the catalytic subunit (37 kDa) could be associated with another polypeptide through disulphide bonds, and that this association could be maintained under some denaturing conditions. This has raised the hypothesis that G6PT might be able to interact with G6PC, resulting in the formation of a complex.

The first aim of the present study was to document the intracellular localisation of G6Pase subunits. The proteins of the G6Pase complex were thus singly labelled on the C or N terminus with cyan fluorescent protein (CFP) for G6PC or yellow fluorescent protein (YFP) for G6PT. We also took advantage of these constructs to test the hypothesis of a direct interaction between both subunits of the G6Pase enzymatic system. To this purpose, we used fluorescence resonance energy transfer (FRET) with CFP as the donor and YFP as the acceptor. The second aim of this work was to test a putative direct interaction between the G6PT cytoplasmic termini. We thus developed a G6PT protein doubly labelled on the C and N termini with CFP and YFP, respectively. Using this chimera protein, we obtained further information on the structural conformation of G6PT within the membrane. Finally, we studied whether the presence

of GSD-1 mutations affected the localisation of both G6Pase subunits and/or the interaction between the C and N termini of the G6PT protein.

2. Materials and methods

2.1 Generation of constructs

We used pSVK3-G6PC and pSVK3-G6PT constructs which contained the coding sequence for human *g6pc* (Genbank number NM 000151) and *g6pt* (Genbank number Y15409) cloned at *EcoRI* and *Sal I* restriction sites (Bady and Mithieux unpublished results). Chimera proteins G6PC-CFP and G6PT-YFP with fluorophores at the C-terminus end were generated introducing *g6pc* and *g6pt* cDNA into pECFP-N1 and pEYFP-N1 vectors (Clontech) at *EcoRI* and *Sal I* restriction sites. Chimera proteins CFP-G6PC and YFP-G6PT with fluorophores at the N-terminus end were generated introducing *g6pc* and *g6pt* cDNA into pECFP-C1 and pEYFP-C1 vectors (Clontech) at *EcoRI* and *Sal I* restriction sites. Sequences encoding stop codons avoiding correct labelling were deleted by mutagenesis (QuikChange, site-directed mutagenesis kit, STRATAGENE). The resulting chimera contained no additional amino acids between the G6PC/G6PT and the CFP/YFP sequences (See supplemental figure 1 for amino acid sequences of the chimera proteins).

In the case of the *CFP-G6PT-YFP* chimera protein, the DNA fragment encoding G6PT-YFP fusion protein was obtained after digestion of pG6PT-YFP plasmid at *XhoI / HpaI* restriction sites. For an easy cloning strategy, this cDNA was inserted to *XhoI / HpaI* in pECFP-Nuc vector. This cloning strategy induced the removal of the nuclear localisation signal of the simian virus large T-antigen contained in the pECFP-Nuc vector and produced a chimera protein containing a linker of 13 amino acids between the CFP and G6PT sequences (See supplemental figure 1).

The sequences of all plasmid constructions were controlled by sequencing (GenomExpress).

2.2 Cell culture and cDNA transfection

HeLa cells (ECACC 85060701), HepG2 cells (ECACC 8511430) and NRK cells (ECACC 86032002) were maintained in Dulbecco's modified Eagle's medium (DMEM; Invitrogen) with 1g/L or 5g/L D-glucose, respectively, and supplemented with 10% foetal bovine serum (Invitrogen), 5 mM glutamine, streptomycin (1µg/µL) and penicillin (1 U/mL) at 37°C in a humidified 5% CO_2/95% air atmosphere. For transient

transfection, 1 day before transfection, 100,000 cells were plated out in two-well cell culture plates (Labteck, NUNC). The complete medium was refreshed 1 h prior to transfection. Cells were transfected using the Exgen 500 reagent (Euromedex) with 200 ng of each construct. After 48 hrs of incubation, the transfection efficiency was about 60% (data not shown).

2.3 Immunoblotting and immunohistochemistry

Whole proteins extracts were prepared from cells homogenised in 10 mM HEPES, pH 7.3 by ultrasonication coupled with freeze-thaw cycles to disrupt cell membranes. Proteins (40 µg) were separated by SDS-10% polyacrylamide electrophoresis gel and then transferred to Immobilon-P membrane (Millipore). Analysis of G6PC expression was performed as previously described using an antibody raised against the C-terminal part of the protein [22].

HepG2 hepatoma cells were fixed with 2% paraformaldehyde in PBS and permeabilised with 0.1% saponin in PBS. The cells were incubated for one hour at room temperature with a G6PC antibody (used at 1:1000) as previously described [22]. The cells were rinsed and then incubated with goat anti-rabbit coupled to Alexa-546 (used at 1:1000, Invitrogen) for 1 h at room temperature.

2.4. Cell microscopy and FRET measurement

Cells were observed using an inverted two-photon laser scanning microscope Axiovert 200M (LSM510 NLO META, Carl Zeiss) equipped with a tunable IR femtosecond Ti:Sa laser (Tsunami, Spectra-Physics). Cells were maintained at 37°C in a humidified atmosphere containing 5% CO_2 using an on-stage incubator (PeCon, Germany). Confocal images of cyan and yellow fluorescence were detected with the emission band-pass filters 480/40 and 535/30 nm, respectively, using an excitation wavelength of 420 nm. Images were acquired using a 63×/1.4 oil immersion objective. Pearson's coefficient was calculated using the JACoP plugin for ImageJ [23].

FRET efficiency in living cells was assessed in confocal mode using the acceptor photobleaching method and using fluorescence lifetime imaging (FLIM) after two-photon excitation. Confocal detection of CFP/YFP was performed using 458/514 nm excitation wavelengths and 480-520/545-610 nm spectral filters, respectively. Repeated scans with unattenuated 514 nm illumination were used to photobleach YFP. After complete YFP bleaching, fluorescence intensities of CFP and YFP were measured

using the same parameters as before photobleaching. FRET efficiency was calculated using the formula E = 1- (I_{DA}/I_D). I is the emission intensity of the donor (CFP) in the presence (I_{DA}) or in the absence (I_D) of the acceptor (YFP). E is the percentage of the increase of the donor fluorescence after bleaching the acceptor. For FLIM, the two-photon laser was tuned to 840 nm with a pulse duration of 150 fs. This wavelength was settled to obtain the best fluorescence excitation of CFP without a noticeable contribution of cellular autofluorescence. The irradiation intensity on the sample was 500 μW at 2% transmission of the acousto-optical tunable filter (AOTF). The fluorescence lifetime of CFP was measured by the time-correlated single photon counting technique (TCSPC) using the counter SPC 830 (Becker & Hickl GmbH, Germany).

2.5. G6Pase activity assay

Cells were homogenised in 10 mM HEPES, pH 7.3 by ultrasonication coupled with freeze-thaw cycles to disrupt cell membranes. Cell extracts were then suspended (1:20 dilution) in 10 mM HEPES and 0.25 M sucrose, pH 7.3. As previously described, we used a specific assay for G6Pase determination, a method involving β-glycerophosphatase activity determinations to determine the contribution of non-specific phosphatase activities from G6Pase activity [3].

3. Results and discussion

3.1 Intracellular localisation of G6Pase subunits.

The intracellular localisation of G6PC and G6PT, obtained from biochemical and histochemical studies, suggested that both proteins localised in the ER membrane [6-8]. However, no recent data based on the detection of G6Pase proteins have confirmed this intracellular localisation. To address this question, we chose to label the cytoplasmic termini of both G6Pase subunits with fluorescent proteins. The predicted model for the G6PC structure suggests that its N terminal part is located on the luminal side of the ER and the C terminal faces the cytoplasm, whereas both termini of G6PT are predicted to be in the cytoplasm (Figure 1 and 2).

The enzymatic activity of G6Pase depends on the integrity of the amino acid sequences of G6PC. Therefore, we first checked that the addition of a fluorophore to the endogenous G6PC protein had no effect on its activity and cellular localisation. Cells transfected with G6PC-CFP (CFP fused the C-terminus of G6PC) conserved notable

G6Pase activity (Figure 1a). This activity was approximately 50% lower than that of cells transfected with the wild-type protein (Figure 1a). This was in agreement with a 50% lower expression of G6PC-CFP compared to G6PC in HeLa cells (Figure 1b). Altogether, this suggested that the fusion of CFP to the C-terminus of G6PC did not substantially alter the intrinsic G6Pase activity of the protein. As previously suggested for the wild-type protein [8], we showed that G6PC-CFP was located in the nuclear membrane and in vesicular structures surrounding the nucleus, which are characteristics of ER membranes (Figure 1c). Surprisingly, G6PC-CFP was also located in punctuate vesicles within the cytoplasm and also close to the surface of the cell (Figure 1c). To confirm that the cellular localisation of the G6PC-CFP construct was the same as the endogenous one, we used an antibody specific for G6PC allowing its detection by immunohistochemistry in G6PC-expressing cells [22]. We showed that endogenous G6PC expressed by the human hepatoma cell line HepG2 exhibited the same intracellular localisation as G6PC-CFP overexpressed in HeLa cells (Figure 1d). Finally, we used a time lapse process, which allowed us to follow up the movement of a point during a determinate time, to determine whether G6PC-CFP fluorescent points were mobile vesicles. We showed that G6PC-CFP expression points moved rapidly (0.5 µm/s) with no orientated trajectory (Movie 1).

Concerning G6PT, the addition of the YFP fluorophore to the C-terminal part of G6PT led to a punctuate pattern in the vicinity of the nucleus similar to that of G6PC-CFP (Figure 2a). Some vesicles were present in the cytoplasm but were localized nearer the nucleus compared to the G6PC-CFP vesicles (Figure 2a). In addition, it must be noted that localisation near the plasma membrane was not observed with G6PT-YFP. Experiment with insertion of the YFP to the N-terminal part of G6PT was also carried out. However, the addition of the YFP fluorophore to the N-terminal part of the protein led to a broader and more diffuse localisation (Figure 2b). YFP is highly hydrophilic. Thus, the presence of the fluorescent protein on the N terminus of G6PT likely perturbed its co-translational insertion process in the ER, thereby explaining the misaddressing of the chimeric protein YFP-G6PT. In agreement with the latter rationale, mutations inducing a destabilisation of G6PT proteins are mainly localised in the N-terminal part and in the first loop of the protein [19]. An exogenous signal peptide could have been added to the N-terminus end of the YFP-G6PT construct in order to force N-terminal insertion in the membrane. However, such a chimera protein might probably not behave as the endogenous G6PT, and results obtained with such a protein

would have been difficult to interpret. For further experiments, we thus used G6PT-YFP chimeras. Finally, using time lapse process, we analysed the behaviour of G6PT-YFP fluorescent points. On the contrary to G6PC-CFP, G6PT-YFP expression points did not move throughout cytoplasm (data not shown).

Both proteins were overexpressed in HeLa cells to analyse their putative colocalisation. The superposition of G6PC-CFP and G6PT-YFP fluorescence patterns suggested that both proteins were colocalised in the perinuclear area (Figure 3c). We calculated the Pearson's coefficient (PC) of correlation to quantify the degree of colocalisation between G6PC-CFP and G6PT-YFP. The PC measures the intensity of fluorescence of each pixel in both channels and compares the channels to determine the amount of correlation. A PC of 1.0 indicates complete colocalisation; a PC of 0 means no correlation and a PC of −1.0 means they are negatively correlated [23]. G6PC-CFP showed a high degree of colocalisation with G6PT-YFP based on PC values of 0.86 ± 0.08 (Figure 3).

To resume, the G6Pase complex was not affected by the labelling of either G6PC or G6PT proteins on their C-termini. Using G6PC-CFP and G6PT-YFP chimera proteins, we demonstrated for the first time that both G6Pase subunits strongly colocalised within the cell. In addition, the presence of G6PC, but nor G6PT within punctuate structures close to the plasma membrane was also detected. We then took advantage of these fluorescent chimeras for investigating a direct interaction between G6Pase subunits.

3.2 Analysis of the interaction between G6PC and G6PT using FRET.

To assess the putative FRET between G6PC-CFP and G6PT-YFP proteins, we determined the energy transfer efficiency by acceptor photobleaching approaches. Acceptor photobleaching approaches with CFP- and YFP-tagged proteins are simple and prevent problems associated with any putative difference in expression levels: when FRET occurs, the fluorescence of the CFP donor increases after bleaching the YFP acceptor chromophore, and this is recognised as a relevant signature for FRET [25].

HeLa cells were transfected with G6PC-CFP and G6PT-YFP proteins and subjected to intense illumination at 514 nm to bleach YFP (100 scans). In the bleached region, we observed a complete loss of yellow fluorescence (compare figure panels 4d with 4b) but no increase in cyan fluorescence (compare figure panels 4a with 4c), indicating the absence of FRET from CFP to YFP before bleaching (Figure 4e). Thus,

these experimental conditions did not allow us to demonstrate the existence of an intermolecular FRET between labelled G6PC and G6PT.

The absence of detected FRET could be due to the cell model used. HeLa cells do not express endogenous G6Pase and could not offer the conditions necessary for an interaction between G6PC and G6PT specific to gluconeogenic cells. To test this hypothesis, we performed the same experiment in a renal cell line (NRK cells, which are able to produce glucose; Soty and Mithieux, unpublished data). However, as in HeLa cells, these experimental conditions did not allow us to demonstrate FRET between G6PC and G6PT (data not shown).

Another explanation for the absence of detectable FRET could be that the rapid movement of G6PC-CFP-labelled vesicles perturbs image acquisition and FRET measurements. Indeed, we showed that G6PC-CFP expression points moved rapidly (0.5 µm/s) (3.1, Movie 1). To detect FRET using acceptor photobleaching approaches, CFP images must be taken before and after YFP photobleaching. Between these two acquisitions, CFP labelled vesicles might disappear or change their localisation due to their putative movements in the x, y or z spatial plans. To test this hypothesis, we performed the detection of FRET by the single photon counting (FLIM), a method insensitive to the variation of fluorescence intensity. FLIM measures the effect of the acceptor on the excited state lifetime of the donor. When FRET is occuring between the donor and the acceptor, the donor lifetime is reduced [26]. The mean lifetime of the double exponential decay of G6PC-CFP was measured to be 1.9 ns in the perinuclear endoplasmic reticulum either in the absence or in the presence of the G6PT-YFP, indicating no FRET between these labels (Supplemental figure 2, white circles). One should notice, however, the strong variation in the G6PC-CFP lifetime values in vesicular structures close to the cell periphery, precluding quantitative FRET analysis using FLIM (Supplemental figure 2).

3.3 Analysis of the interaction between G6PT termini.

The predicted model for the G6PT structure suggests that G6PT is anchored in the ER membrane by 10 transmembrane helices and has both termini facing the cytoplasm [19]. The interaction between these termini has not been addressed yet. To study the conformational behaviour of G6PT ends, we generated a G6PT protein tagged on the C and N termini with CFP and YFP, respectively (CFP-G6PT-YFP).

The intracellular distribution of the doubly labelled G6PT subunit (CFP-G6PT-YFP protein) was similar to the simply labelled subunit G6PT-YFP (Figure 5a, b). After YFP fluorescence extinction under the conditions previously described (3.2), we showed an increase in cyan fluorescence, demonstrating the existence of a FRET phenomenon between CFP and YFP before bleaching (compare figure panels 5a with 5c). The ratio of the YFP/CFP fluorescence intensities was constant and not correlated with FRET efficiency. This observation illustrated that the labelling stoichiometry was 1:1 and that both fluorophores were never expressed independently (Figure 5e) [27]. The mean intramolecular FRET efficiency of the CFP-G6PT-YFP protein was 27%. This result indicates that the G6PT protein adopted a wrapped conformation, so that FRET occurred between its two extremities [27]. From these data, we estimated the distance between the C and N termini of G6PT to 5.8 nm (supposing the Förster radius for CFP/YFP pair is 4.9 nm [28]).

Some data [15, 29] have argued for the existence of a direct influence of G6PC protein on G6PT transport function. We tested the hypothesis that the presence of unlabelled G6PC could induce a conformational change to the CFP-G6PT-YFP chimera detectable by a modification of its FRET efficiency. The co-expression of unlabelled G6PC with CFP-G6PT-YFP in HeLa cells did not modify the FRET efficiency of the doubly labelled G6PT (23.64 ± 6.29 vs. 25.61 ± 9.86%). These results suggest that G6PC did not modify the interaction between G6PT termini.

3.4 Effect of GSD-1 mutations on G6Pase subunit intracellular localisation and on G6PT intramolecular FRET.

Mutations identified in GSD-1 patients have been studied *in vitro* to assess their effect on protein stability and enzymatic activity [18, 19, 30]. From these data, we selected mutations located in different parts of G6PC or G6PT which did not affect the stability of the proteins but annulled or strongly decreased their enzymatic activity (Table 1) [30]. Our fluorescent chimera enabled us for the first time to test whether the decrease of G6Pase activity due to GSD-1 mutations was linked to a cellular mislocalisation of G6Pase subunits. Concerning G6PC, we introduced some GSD-1a mutations on the G6PC-CFP construct (E110K, A241T, G184R and G222R). We did not observe an effect of any of these mutations on the cellular localisation of G6PC-CFP. As an example, the E110K mutation, which induced a complete loss of G6Pase activity (Table 1) [30], exhibited the same localisation pattern as the wild-type protein

(Figure 6b). Concerning G6PT, we introduced some GSD-1b mutations in the CFP-G6PT-YFP construct (S54R, H301P, and A367T). We did also not observe an effect of any of these mutations on the cellular localisation of G6PT-YFP. Indeed, the S54R mutation, which induced a complete loss of G6Pase activity, or the H301P mutation, which kept about 25% of wild type G6Pase activity (Table 1) [30], exhibited the same localisation pattern as the wild type CFP-G6PT-YFP construct (Figure 6c-h).

GSD-1b disease is characterised by the loss of G6Pase activity due to G6P transport deficiency [24]. In addition to defects in glucose homeostasis, GSD-1b patients present symptoms of neutropenia and myeloid dysfunction [31]. These data are consistent with the idea that G6PT is not just a G6Pase partner but also a key protein for normal neutrophil function. Therefore, knowledge of G6PT structure-function relationships could be crucial for the understanding of both G6Pase function and GSD-1b pathophysiology. To identify whether the loss of function of G6PT observed in GSD-1b patients is associated with a spatial rearrangement between its C and N termini, we tested the influence of some GSD-1b mutations on the FRET efficiency of CFP-G6PT-YFP. However, the presence of the selected mutations did not affect the FRET efficiency of the CFP-G6PT-YFP construct (Figure 7). In summary, our results strongly suggest that the decrease or the loss of G6Pase activity in GSD1 patients was not linked to a mislocalisation of any G6Pase subunits or to an alteration of the interaction between G6PT termini.

4. Conclusion

In conclusion, this study constitutes an original focus on the intracellular distribution of G6PC and G6PT. We suggest that both proteins are strikingly co-localised in the intracellular membranes close to the nucleus. Moreover, G6PC, but not G6PT, is also present in vesicles throughout the cytoplasm and is subject to rapid motion within the cell. For the first time, our results demonstrated that G6PT C and N-termini are separated by about 5-6 nm strongly suggesting that G6PT adopts within the ER membrane a wrapped conformation. Moreover, the intramolecular interactions are strong enough for the G6PT conformation be maintained either in the presence of G6PC or in the presence of mutations identified in GSD-1b patients.

Proprietary interest

None.

Acknowledgements

The authors thank INSERM for funding their work, as well as CNRS (G.M.), INRA (A.G.-S.) and the French Ministry of Research (M.S., J.C. and S.C.) for funding their positions.

References

[1] Ashmore, J., A.B. Hastings, F.B. Nesbett, and A.E. Renold, Studies on carbohydrate metabolism in rat liver slices. VI. Hormonal factors influencing glucose-6-phosphatase. J. Biol. Chem. 218 (1956) 77-88.

[2] Wirthensohn, G. and W.G. Guder, Renal substrate metabolism. Physiol. Rev. 66 (1986) 469-97.

[3] Rajas, F., N. Bruni, S. Montano, C. Zitoun, and G. Mithieux, The glucose-6 phosphatase gene is expressed in human and rat small intestine: regulation of expression in fasted and diabetic rats. Gastroenterology 117 (1999) 132-9.

[4] Chen, Y.T., Glycogen storage diseases, in Scriver CR, Beaudet AL, Sly WS, Valle D (Eds.) The Metabolic and Molecular Basis of Inherited Disease, 8th ed. McGraw-Hill Inc, New York, 2001 pp. 1521-1551.

[5] Arion, W.J., A.J. Lange, H.E. Walls, and L.M. Ballas, Evidence for the participation of independent translocation for phosphate and glucose 6-phosphate in the microsomal glucose-6-phosphatase system. Interactions of the system with orthophosphate, inorganic pyrophosphate, and carbamyl phosphate. J. Biol. Chem. 255 (1980) 10396-406.

[6] Arion, W.J., B.K. Wallin, P.W. Carlson, and A.J. Lange, The specificity of glucose 6-phosphatase of intact liver microsomes. J Biol Chem, 247 (1972) 2558-65.

[7] Chiquoine, A.D., The distribution of glucose-6-phosphatase in the liver and kidney of the mouse. J. Histochem. Cytochem. 1 (1953) 429-35.

[8] Shin, T.S., I.H. Chung, and S.S. Kim, Electron microscopy on activity and localization of glucose-6-phosphatase in liver cells. Yonsei Med J, 19 (1978) 1-10.

[9] van Schaftingen, E. and I. Gerin, The glucose-6-phosphatase system. Biochem. J. 362 (2002) 513-32.

[10] Veiga-da-Cunha, M., I. Gerin, and E. Van Schaftingen, How many forms of glycogen storage disease type I ? Eur. J. Pediatr. 159 (2000) 314-8.

[11] Arion, W.J., B.K. Wallin, A.J. Lange, and L.M. Ballas, On the involvement of a glucose 6-phosphate transport system in the function of microsomal glucose 6-phosphatase. Mol. Cell. Biochem. 6(1975) 75-83.

[12] Mithieux, G., New knowledge regarding glucose-6 phosphatase gene and protein and their roles in the regulation of glucose metabolism. Eur. J. Endocrinol. 136 (1997) 137-45.

[13] Burchell, A., Molecular pathology of glucose-6-phosphatase. Faseb J. 4 (1990) 2978-88.

[14] Narisawa, K., Y. Igarashi, H. Otomo, and K. Tada, A new variant of glycogen storage disease type I probably due to a defect in the glucose-6-phosphate transport system. Biochem. Biophys. Res. Commun. 83 (1978) 1360-4.

[15] Lei, K.J., H. Chen, C.J. Pan, J.M. Ward, B. Mosinger, Jr., E.J. Lee, H. Westphal, B.C. Mansfield, and J.Y. Chou, Glucose-6-phosphatase dependent substrate transport in the glycogen storage disease type-1a mouse. Nat. Genet. 13 (1996) 203-9.

[16] Chou, J.Y., A. Zingone, and C.J. Pan, Adenovirus-mediated gene therapy in a mouse model of glycogen storage disease type 1a. Eur J Pediatr. 161 Suppl 1 (2002) S56-61.
[17] Hiraiwa, H., C.J. Pan, B. Lin, S.W. Moses, and J.Y. Chou, Inactivation of the glucose 6-phosphate transporter causes glycogen storage disease type 1b. J Biol Chem. 274 (1999) 5532-6.
[18] Pan, C.J., K.J. Lei, B. Annabi, W. Hemrika, and J.Y. Chou, Transmembrane topology of glucose-6-phosphatase. J Biol Chem. 273 (1998) 6144-8.
[19] Pan, C.J., B. Lin, and J.Y. Chou, Transmembrane topology of human glucose 6-phosphate transporter. J Biol Chem. 274 (1999) 13865-9.
[20] Daniele, N., F. Rajas, B. Payrastre, G. Mauco, C. Zitoun, and G. Mithieux, Phosphatidylinositol 3-kinase translocates onto liver endoplasmic reticulum and may account for the inhibition of glucose-6-phosphatase during refeeding. J Biol Chem. 274 (1999) 3597-601.
[21] Ness, G.C., K.A. Sukalski, C.E. Sample, L.C. Pendleton, M.J. McCreery, and R.C. Nordlie, Radiation inactivation analysis of rat liver microsomal glucose-6-phosphatase. J Biol Chem. 264(1989) 7111-4.
[22] Rajas, F., H. Jourdan-Pineau, A. Stefanutti, E.A. Mrad, P.B. Iynedjian, and G. Mithieux, Immunocytochemical localization of glucose 6-phosphatase and cytosolic phosphoenolpyruvate carboxykinase in gluconeogenic tissues reveals unsuspected metabolic zonation. Histochem. Cell. Biol. 127 (2007) 555-65.
[23] Bolte, S. and F.P. Cordelieres, A guided tour into subcellular colocalization analysis in light microscopy. J Microsc, 224 (2006) 213-32.
[24] Chou, J.Y., The molecular basis of type 1 glycogen storage diseases. Curr Mol Med. 1 (2001) 25-44.
[25] Sekar, R.B. and A. Periasamy, Fluorescence resonance energy transfer (FRET) microscopy imaging of live cell protein localizations. J Cell Biol. 160(2003) 629-33.
[26] Hayek, A., A. Grichine, T. Huault, C. Ricard, F. Bolze, B. Van Der Sanden, J.C. Vial, Y. Mely, A. Duperray, P.L. Baldeck, and J.F. Nicoud, Cell-permeant cytoplasmic blue fluorophores optimized for in vivo two-photon microscopy with low-power excitation. Microsc Res Tech. 70 (2007) 880-5.
[27] Hink, M.A., T. Bisselin, and A.J. Visser, Imaging protein-protein interactions in living cells. Plant Mol Biol. 50 (2002) 871-83.
[28] Patterson, G.H., D.W. Piston, and B.G. Barisas, Forster distances between green fluorescent protein pairs. Anal Biochem. 284 (2000) 438-40.
[29] Sloop, K.W., A.D. Showalter, A.L. Cox, J.X. Cao, A.M. Siesky, H.Y. Zhang, A.R. Irizarry, S.F. Murray, S.L. Booten, E.A. Finger, R.A. McKay, B.P. Monia, S. Bhanot, and M.D. Michael, Specific Reduction of Hepatic Glucose 6-Phosphate Transporter-1 Ameliorates Diabetes while Avoiding Complications of Glycogen Storage Disease. J Biol Chem. 282 (2007) 19113-21.
[30] Shieh, J.J., M. Terzioglu, H. Hiraiwa, J. Marsh, C.J. Pan, L.Y. Chen, and J.Y. Chou, The molecular basis of glycogen storage disease type 1a: structure and function analysis of mutations in glucose-6-phosphatase. J Biol Chem. 277 (2002) 5047-53.
[31] Beaudet, A.L., D.C. Anderson, V.V. Michels, W.J. Arion, and A.J. Lange, Neutropenia and impaired neutrophil migration in type IB glycogen storage disease. J Pediatr. 97(1980) 906-10.

Figure legends

Figure 1: Characteristics of the G6PC chimera.
HeLa cells were transfected with the empty pSVK3 plasmid (mock) or with plasmids coding for the human wild-type G6PC or coding for G6PC-CFP. **a.** G6Pase activities assayed in the lysates of transfected HeLa cells. Results are expressed as means ± SEM (n=4).* P<0.05, significantly different from mock value (Student's t-test for unpaired data). **b.** Representative immunoblot for G6PC illustrating the sizes of the wild-type and chimera G6PC proteins. Molecular weight of the protein marker is indicated on the right of the figure. **c,d**. Representative confocal images of (**c**) G6PC-CFP in HeLa cells (**d**) endogenous G6PC in HepG2 cells. Bar = 10µm

Figure 2: Characteristics of the G6PT-CFP constructs.
Representative confocal images of (**a**) G6PT-YFP and (**b**) YFP-G6PT expressed in HeLa cells. Bar = 10µm

Figure 3: Colocalisation of the G6PC and G6PT chimeras.
Representative confocal images of (**a**) G6PC-CFP by CFP excitation and (**b**) G6PT-YFP by YFP excitation in HeLa cells transiently expressing a 1:1 ratio of G6PC-CFP and G6PT-YFP constructs. (**c**) Overlay of CFP and YFP emissions from the same cells. Bar = 10µm. Pearson's coefficients (mean of eight independent experiments) indicate the degree of colocalisation between both chimera.

Figure 4: Photobleaching of yellow fluorescence associated with G6PT-YFP in HeLa cells.
Representative images of G6PC-CFP (**a,c**) and G6PT-YFP (**b,d**) co-expressed in HeLa cells. The images were acquired immediately before (**a, b***)* and after (**c, d***)* bleaching (see 2.4 for details). The bleached region is delimited by a white circle. Bar = 10µm. **e.** Pixel intensities of CFP fluorescence acquired before and after photobleaching. Results represent the mean ± SD of eight independent experiments.

*Figure 5: Photobleaching of yellow fluorescence associated with CFP-G6PT-YFP***.**
Confocal imaging of cyan (**a, c**) and yellow (**b, d**) fluorescence of CFP-G6PT-YFP expressed in HeLa cells. The images were acquired immediately before (**a, b**), and after (**c, d**) bleaching. The bleached region is delimited by a white circle. Bar = 10µm **e.** FRET efficiencies (y) (see 2.4 for calculation) for doubly labelled G6PT according to the ratio of corrected fluorescence intensities for CFP and YFP (x).

Figure 6: Effect of GSD-1 mutations on G6Pase subunit localisation.
Representative confocal images of wild-type (**a**) and E110K (**b**) G6PC-CFP in HeLa cells. Representative confocal images of cyan (left panels) and yellow (right panels) fluorescence of wild-type (**c, d**), S54R (**e, f**) or H301P (**g, h**) CFP-G6PT-YFP constructs in HeLa cells. Bar = 10µm.

Figure 7: Effect of GSD-1b mutations on FRET efficiency of CFP-G6PT-YFP.
FRET efficiency was calculated as previously described. Results are expressed as means ± SEM (n =3).

Table 1: GSD-1 mutations used in the study

GSD-1 mutations located in loops of G6PC and G6PT, with no effect on protein stability or G6Pase activity were chosen. Table indicates the amino acids targeted by the mutation, its localisation on the predicted model of the protein and its effect on G6Pase activity compared to wild type [18, 19, 30].

Movie 1 (MOV file): HeLa cells were transfected with the G6PC-CFP construct. Confocal images of cyan fluorescence were detected with the emission band-pass filters 480/40 nm using an excitation wavelength of 420 nm. Images were acquired using a 63×/1.4 oil immersion objective every sec for over 70 sec.

Movie 2 (MOV file): HeLa cells were transfected with the G6PT-YFP construct. Confocal images of yellow fluorescence were detected with the emission band-pass filters 535/30 nm using an excitation wavelength of 514 nm. Images were acquired using a 63×/1.4 oil immersion objective every 0.4 sec for over 85 sec.

Supplemental material

Supplemental Figure 1: Amino acid sequences of the chimera proteins used in this study.

Underlined texts correspond to the CFP or YFP sequences. Texts highlighted in grey correspond to G6PC or G6PC sequences. Nucleic acids coding for the stop codon of G6PC (**A**), G6PT (**B**), CFP (**C**) or YFP (**D**) and nucleic acids from the cloning vector located between G6PC and CFP (**A and C**) or between G6PT and YFP (**B and D**) were removed by site-directed mutagenesis. **E.** Nucleic acids coding for the nuclear localisation signal from simian virus large T-antigen contained in the pECFP-Nuc vector were removed by the cloning strategy.

Supplemental Figure 2: Analysis of the G6PC-CFP and G6PT-YFP interaction using FRET- FLIM.

G6PC-CFP lifetimes measured by the TCSPC method in HeLa cells co-expressing G6PC-CFP and G6PT-YFP are represented before (**a**), and after (**b**) bleaching (see 2.4 for details). The bleached region is delimited by a white circle. Lifetime is indicated by the color bar.

Table 1

Amino acid changes	Location	Effect on G6Pase activity
GSD-1a mutations		
E110K	1st Loop	Total inactivation
A241T	3rd loop	21.3 % of wild type activity
G184R	5th loop	Total inactivation
G222R	6th loop	4 % of wild type activity
GSD-1b mutations		
S54R	1st Loop	Total inactivation
H301P	3rd loop	24.2 % of wild type activity
A367T	9th loop	23.1 % of wild type activity

Table 1: GSD-1 mutations used in the study

Table 1, Soty et al.

Figure1

Click here to download high resolution image

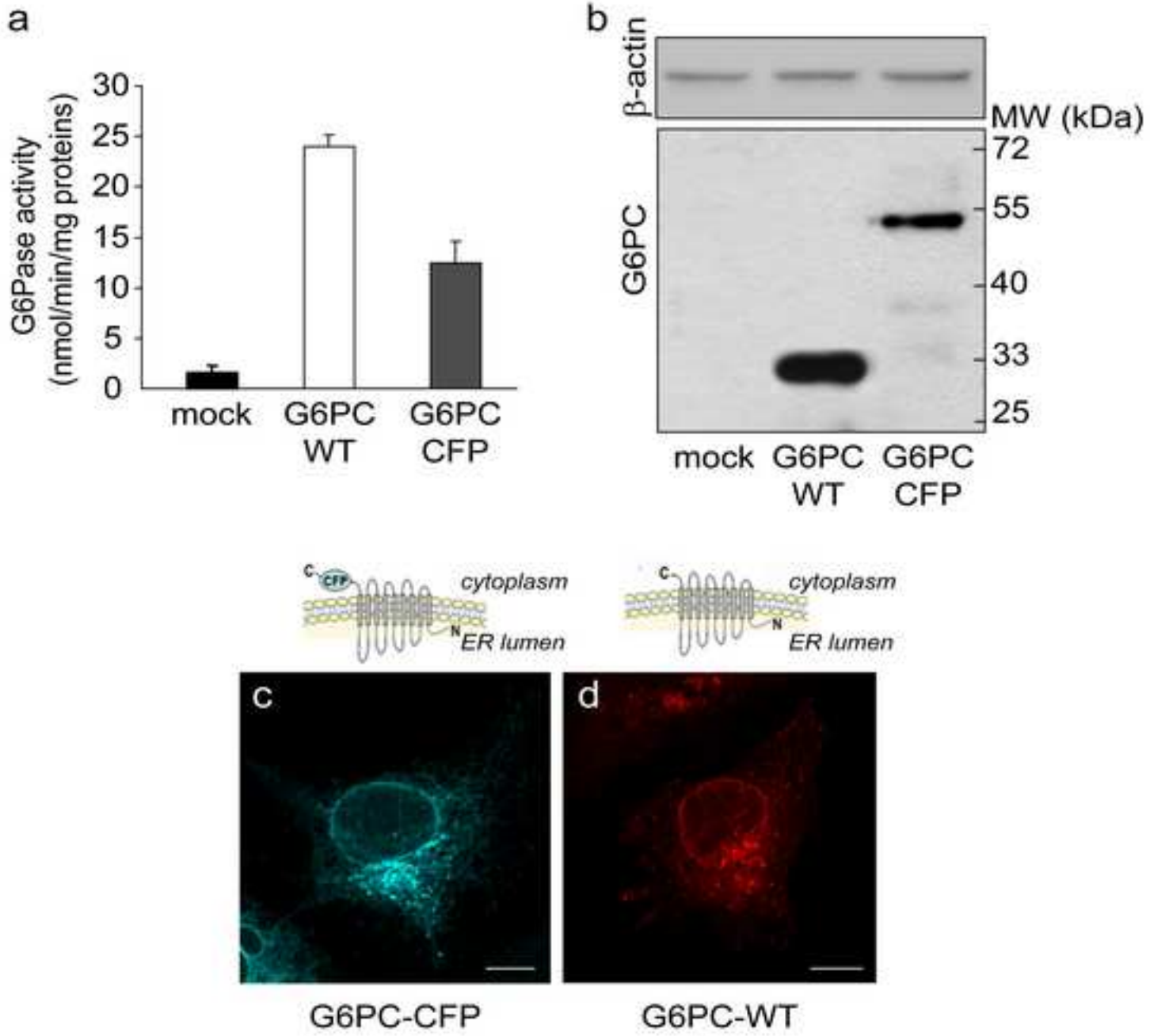

Figure 1, Soty et al.

Figure2

Click here to download high resolution image

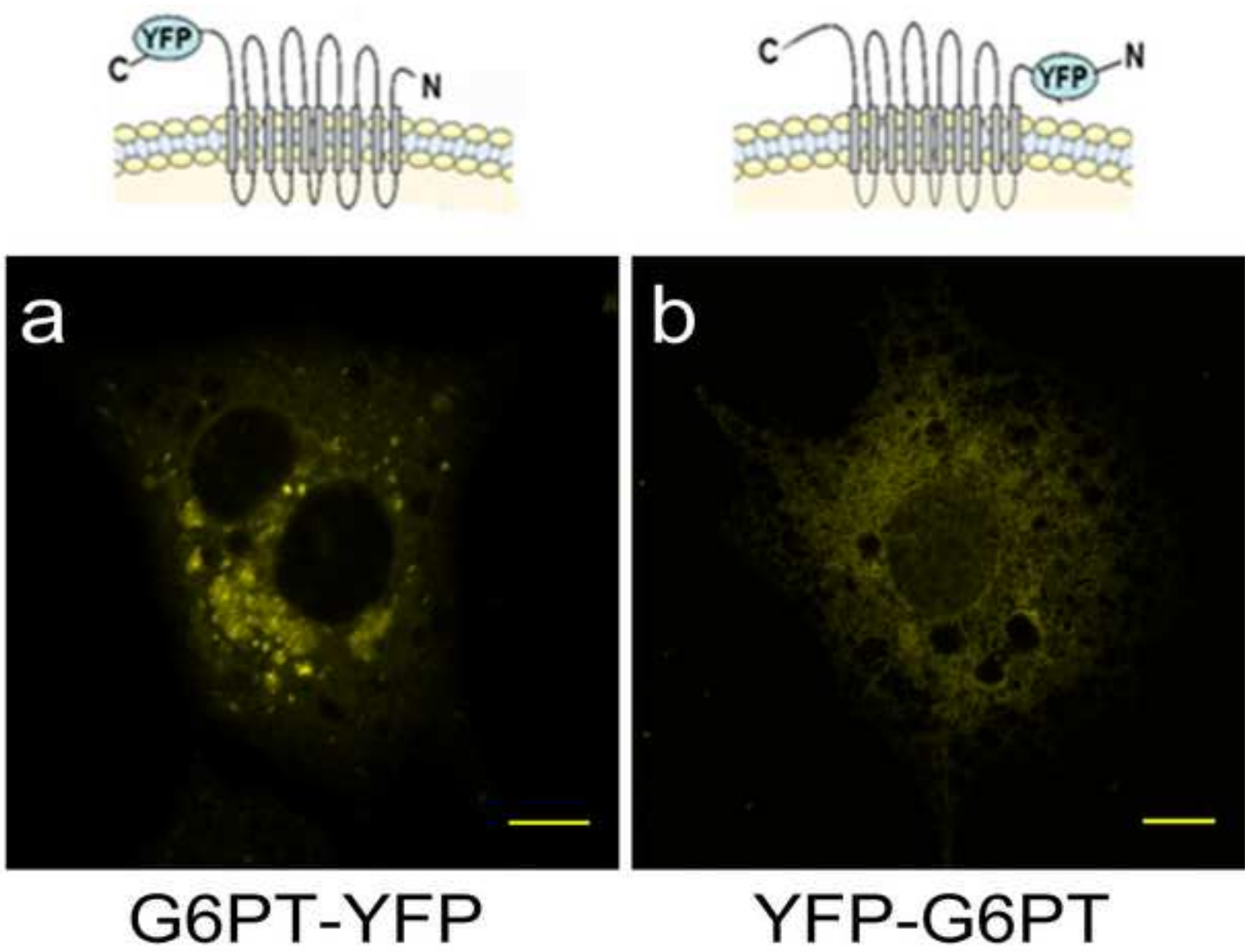

Figure 2, Soty et al.

Figure3
Click here to download high resolution image

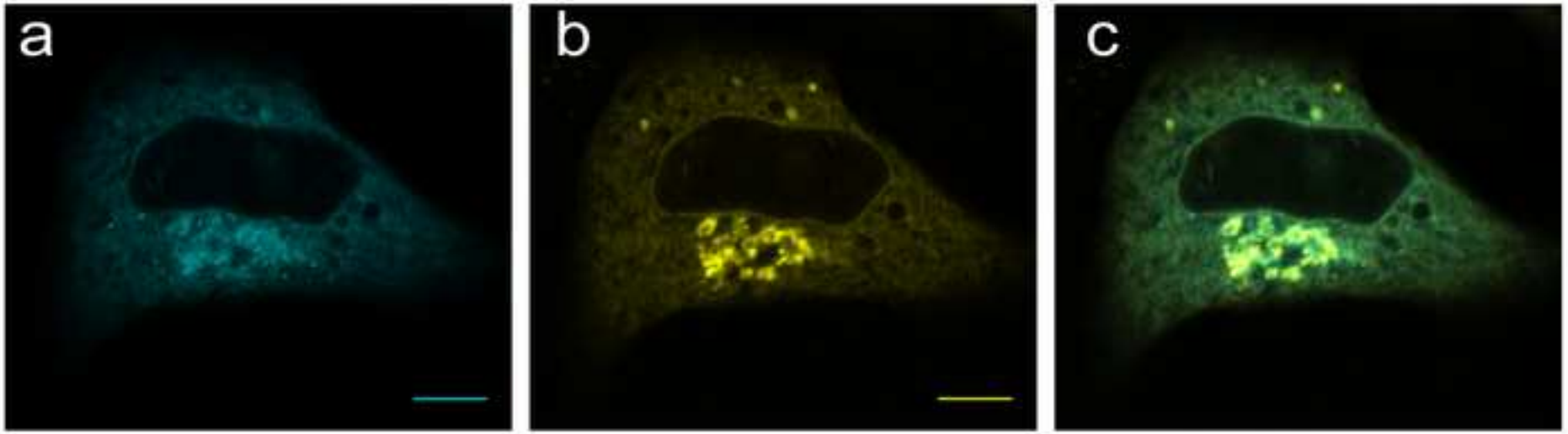

Pearson coeff = 0.86 ± 0.08 (n=4)

Figure 3, Soty et al.

Figure4
Click here to download high resolution image

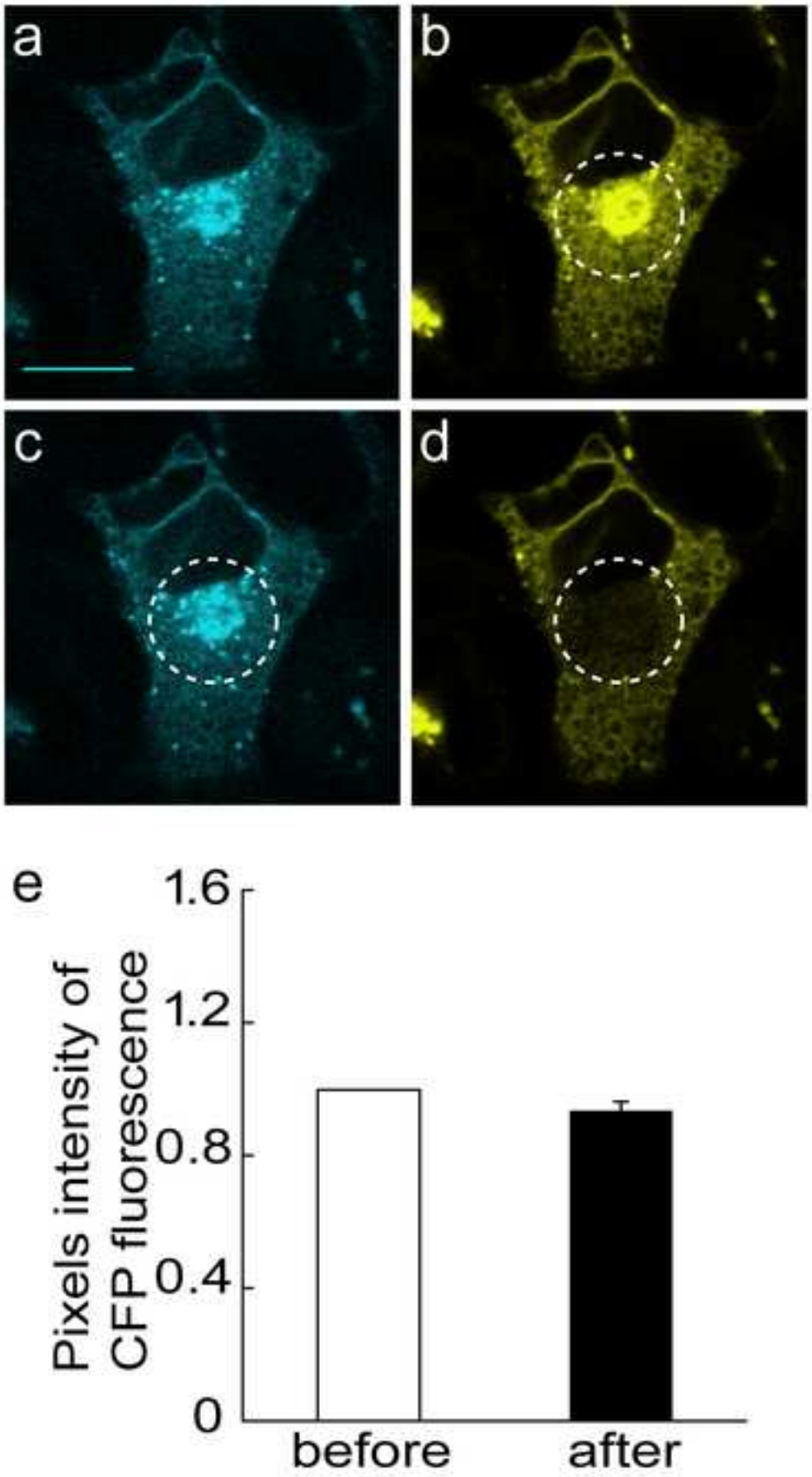

Figure 4, Soty et al.

Figure 5

Click here to download high resolution image

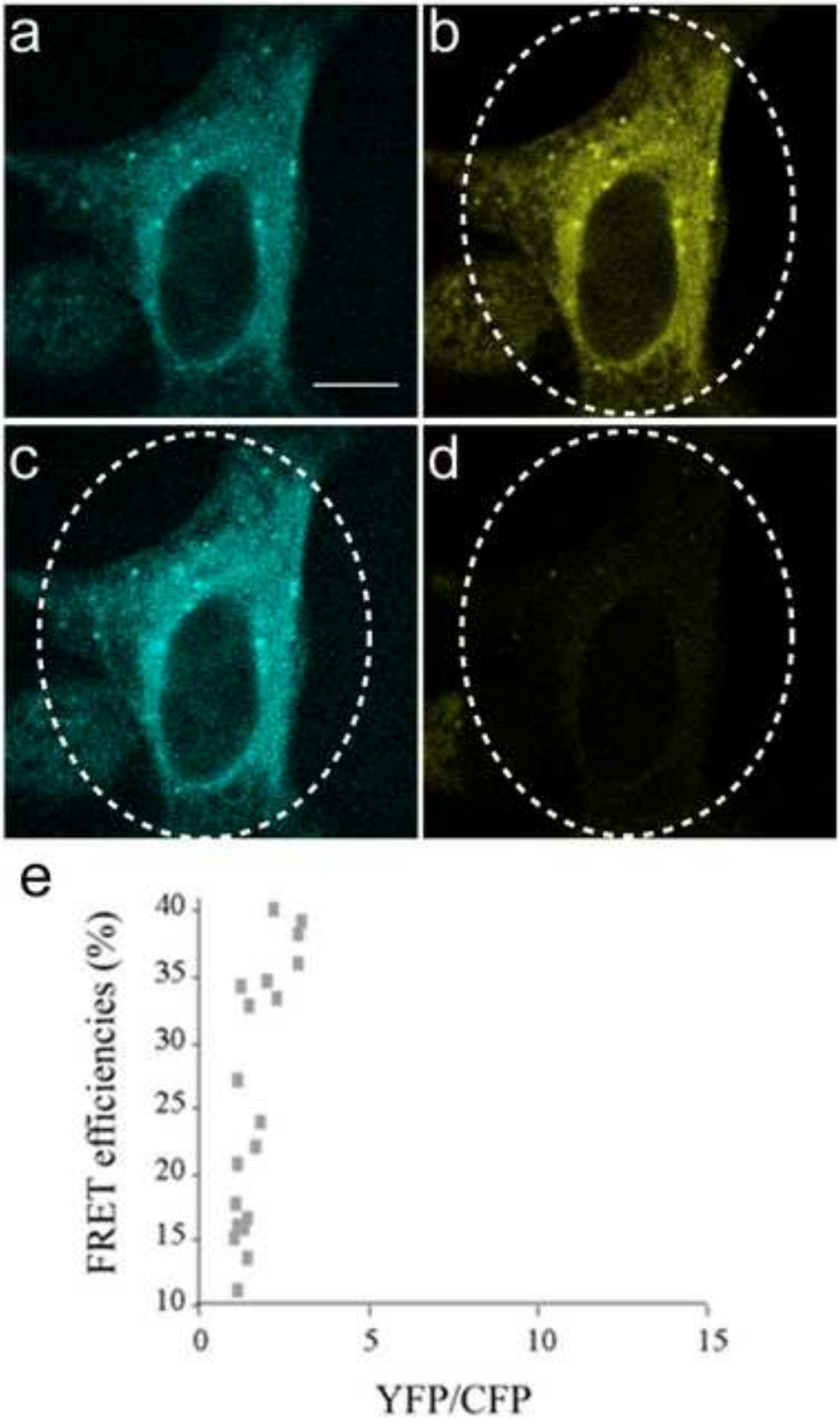

Figure 5, Soty et al.

Figure 6

Click here to download high resolution image

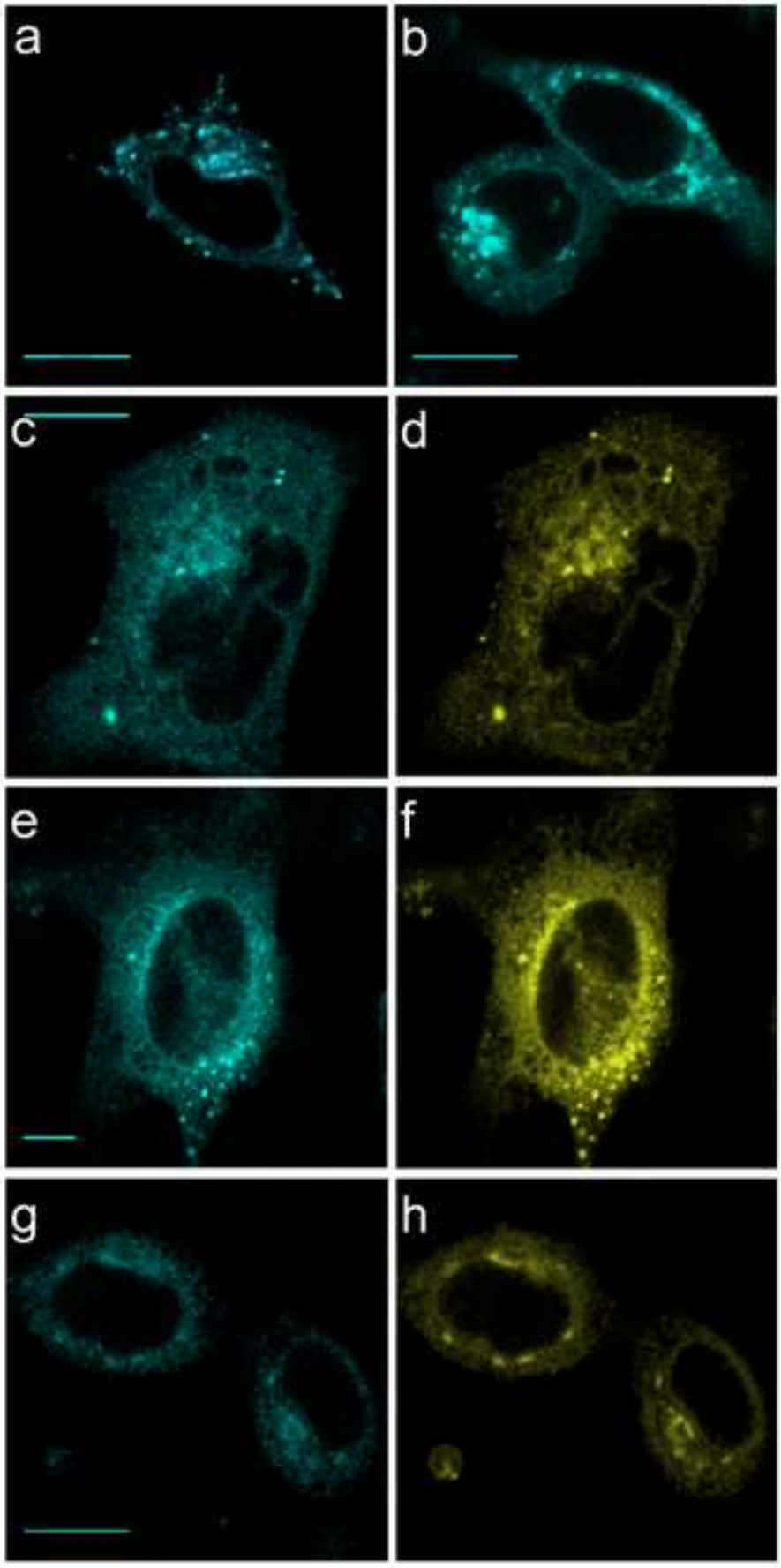

Figure 6, Soty et al.

Figure 7
Click here to download high resolution image

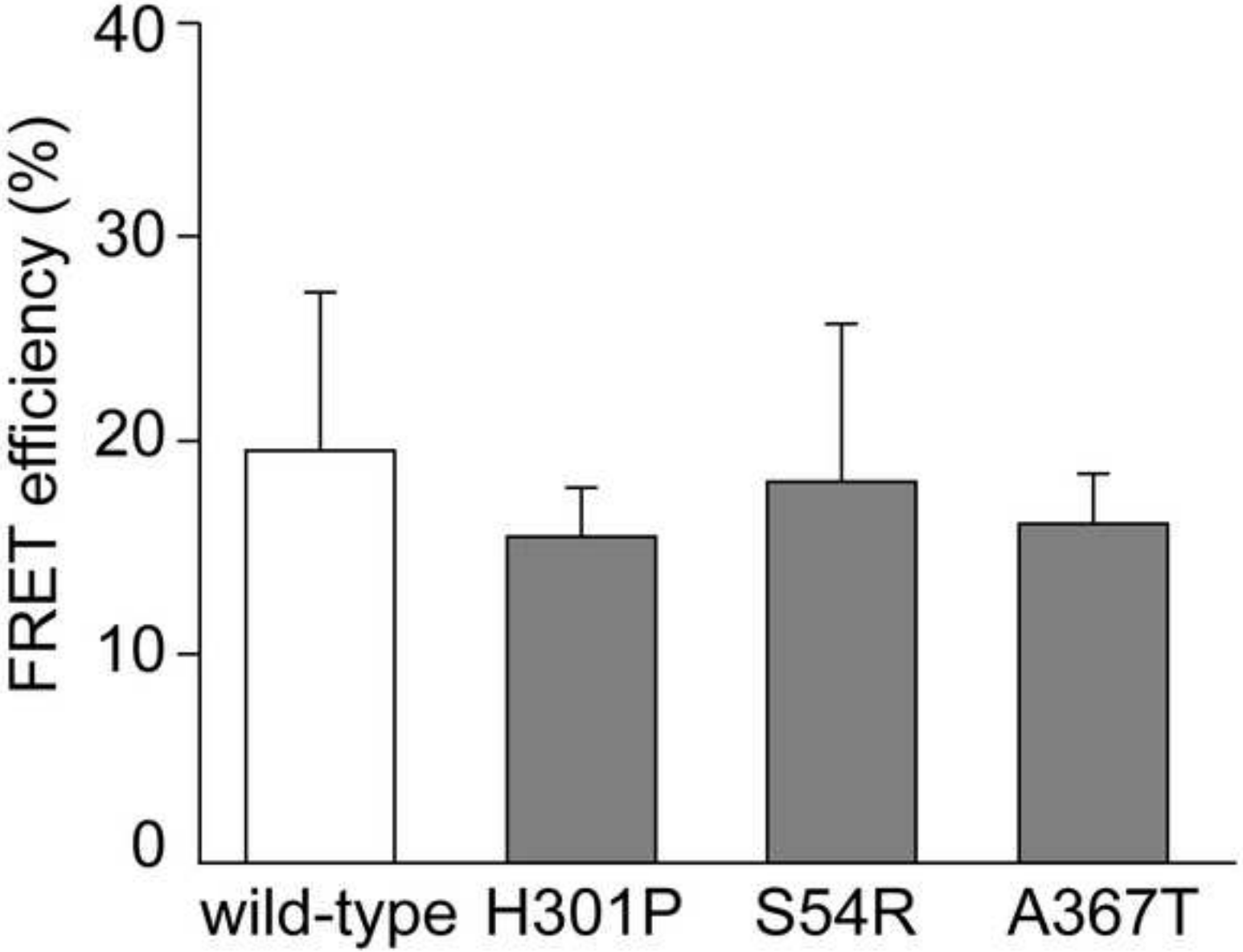

Figure 7, Soty et al.

Supplemental figure 1

Click here to download Supplementary Material: Supplemental Figure 1.doc

Supplementary figure 2

Click here to download Supplementary Material: supplemental figure 2.tif

movie1

Click here to download Video: movie.mov

movie2

Click here to download Video: movie2.mov